



An integrated data analysis tool for improving measurements on the MST RFP^{a)}

^{a)} Contributed paper, published as part of the Proceedings of the 20th Topical Conference on High-Temperature Plasma Diagnostics, Atlanta, Georgia, USA, June 2014.

L. M. Reusch^{1,b)}, M. E. Galante¹, P. Franz², J. R. Johnson¹, M. B. McGarry¹, H. D. Stephens^{1,3} and D. J. Den Hartog¹

b) Electronic mail: Immcguire@wisc.edu

Rev. Sci. Instrum. 85, 11D844 (2014); <http://dx.doi.org/10.1063/1.4886957>

Abstract

Many plasma diagnostics contain complementary information. For example, the double-foil soft x-ray system (SXR) and the Thomson Scattering diagnostic (TS) on the Madison Symmetric Torus both measure electron temperature. The complementary information from these diagnostics can be combined using a systematic method based on integrated data analysis techniques, leading to more accurate and sensitive results. An integrated data analysis tool based on Bayesian probability theory was able to estimate electron temperatures that are consistent with both the SXR and TS diagnostics and more precise than either. A Markov Chain Monte Carlo analysis to increase the flexibility of the tool was implemented and benchmarked against a grid search method.

Key Topics

Soft X-rays

Plasma diagnostics

Probability theory

Temperature

measurement

Data analysis

The extreme plasma environments in next step fusion devices such as ITER will limit diagnostic data. Integrated data analysis (IDA) is a method for combining limited data from multiple diagnostics, along with their uncertainties, to extract common parameter(s) of interest. This method has been implemented

on a number of plasma fusion experiments to measure a variety of parameters (see Refs. 1–3 for some examples). On the Madison Symmetric Torus (MST) reversed field pinch (RFP), the double-foil soft x-ray (SXR) tomography and Thomson Scattering (TS) diagnostics both contain information about electron temperature (T_e). A traditional analysis approach is to analyze the data sets separately, extract the temperature calculated by each one, and compare them; however, this neither addresses issues that arise if and when the diagnostics disagree, nor does it leverage the wealth of information that they jointly contain. Using IDA techniques to combine the data from separate diagnostics while extracting T_e overcomes both of those problems. The result is consistent with the data from all the diagnostics included, and the precision is improved due to the fact that there are more independent measurements. In this paper, we present the initial development of an IDA tool using Bayesian probability theory (BPT) for MST, concentrating on T_e using SXR and TS.

Bayesian probability theory is a useful framework with which to pursue IDA due to its modularity, reliance only on forward models, and its ability to include background information into the calculation of a parameter. The core of BPT is Bayes' rule:⁴

$$P(x|Data, I) = \frac{P(Data|x, I)P(x|I)}{P(Data|I)},$$

(1)

where $P(x|Data, I)$, the posterior probability, is the conditional probability of getting a particular value for the parameter of interest x , given the data and any background information I . $P(Data|x, I)$, called the likelihood function, is the probability of getting the data given a particular value for x and any background information. $P(x|I)$, the prior probability, represents any prior knowledge we have about the value of x . Finally, $P(Data|I)$, called the evidence, is a normalization constant that gives the absolute probability. Making the assumption that the TS and SXR measurements are completely independent when combining them, Bayes' rule takes the form

$$P(\vec{a}|\vec{SXR}, \vec{TS}, I) \propto \prod_i P(SXR_i|\vec{a}, I) \\ \times \prod_j P(TS_j|\vec{a}, I) \prod_k P(a_k|I),$$

(2)

where \vec{a} is a vector containing the desired fit parameters, \vec{SXR} and \vec{TS} denote a set of experimental data from SXR and TS, respectively, and I is the background information. $P(SXR_i|\vec{a}, I)$ and $P(TS_j|\vec{a}, I)$ are the likelihood functions for the i th SXR chord and j th TS point, respectively, and $P(a_k|I)$ describes the prior information we have about the desired fitting parameters.

The other primary tool in BPT, marginalization, can be used in the case where there are multiple parameters. Marginalization is given by

$$P(x|Data, I) = \int P(x, y|Data, I) dy,$$

(3)

where the integral is taken over all possible values for y . In this case, y is said to be “marginalized” to give the probability of getting a particular value for parameter x , regardless of the exact value of y .⁴

The double-foil SXR tomography system on MST has 40 unique viewing chords arranged such that they cover a 2-dimensional poloidal cross-section of the plasma. Each viewing chord is equipped with two detectors, a 421 μm beryllium filter and a 857 μm beryllium filter. Further details on the diagnostic can be found in Refs. 5,6. The analysis is based on the double-foil technique, which uses the ratio of brightnesses from detectors that share a line of sight to find the temperature.^{7,8} We ascribe a gaussian to the SXR likelihood function:

$$P(\text{SXR}_i | \vec{a}, I) = \frac{1}{\sigma_{\text{SXR},i} \sqrt{2\pi}} \exp \left[\frac{-(R_{m,i} - R_{c,i})^2}{2\sigma_{\text{SXR},i}^2} \right],$$

(4)

where $R_{m,i}$ and $R_{c,i}$ are the measured and calculated ratios of i th SXR chord, respectively. The uncertainty $\sigma_{\text{SXR},i}$ includes both the measured electronic noise and systematic uncertainties. We calculate the systematic uncertainties include a relative uncertainty of about 2% of the measured brightness that takes into account uncertainty in detector position and size, exact filter thickness, and solid angle of the probe.⁹

The value for $R_{c,i}$ is generated by an existing soft x-ray model that calculates theoretical x-ray emissivity, expected brightness given the behavior of the filters and detector diodes, and, ultimately, brightness ratio for each chord using a specified temperature.¹⁰ Specifically, the model takes as input a radial profile for temperature, which, in the absence of any temperature structures, can be parameterized as

$$T_e(r/a) = T_{e0} (1 - (r/a)^\alpha)^\beta,$$

(5)

where T_{e0} is the core temperature and r/a is the normalized radius. The three parameters, T_{e0} , α , and β make up vector \vec{a} .

MST is also equipped with a 21-chord Thomson Scattering diagnostic covering from the core to the edge of MST.¹¹ The temperature analysis of the TS diagnostic already uses a BPT framework,¹² however, to be consistent with the SXR analysis, we find the best fit of T_e measured by TS to a profile given by Eq. (5) where r/a takes the value of the locations of the TS measurement points. We approximate the TS likelihood as gaussian, and use

$$P(TS_j | \vec{a}, I) = \frac{1}{\sigma_{TS,j} \sqrt{2\pi}} \exp \left[\frac{-(T_{m,j} - T_{c,j})^2}{2\sigma_{TS,j}^2} \right]$$

(6)

for the TS likelihood function, where \vec{a} contains the same parameters as for the SXR likelihood, and $T_{m,j}$, $T_{c,j}$ and $\sigma_{TS,j}$ are the measured and calculated temperatures and uncertainty of the j th TS point, respectively.

In general, all we know about each parameter is a range of possible values, but we have no reason to choose one value over another within that range. Thus, the prior probability for each parameter is a uniform distribution over the respective ranges and zero outside of it. Temperature must be positive, so Te_0 must be greater than zero and, in principle, can have any positive value. Since the hottest electron temperatures typically measured in experiment are usually ~ 1500 eV, we use an upper bound of 2000 eV so that our range is finite. In experiment, we generally see α values of between 7 and 12 and β values between 4 and 19.

To characterize the integration technique, we first generate a set of synthetic ratio data ($R_{m,i}$) and $Te(r/a)$ for TS ($T_{m,j}$) with $Te_0 = 1350$ eV, $\alpha = \beta = 8$. Analysis is done using 3-dimensional (3D) grids of pre-calculated theoretical ratios for $R_{c,i}$ for SXR and Te profiles for TS ($T_{c,j}$), generated by systematically varying Te_0 , α , and β over the range specified by the priors. Using Eqs. (4) and (6) and uncertainties based on experimental measurements, we calculate the likelihoods for the synthetic SXR data and TS data separately. The posterior probability is given by combining the two likelihood functions and the priors. The result is a 3D array of probabilities describing the probability that each combination of Te_0 , α , and β gave rise to both sets of data. The plots in Figs. 1(a)–1(c) show the distribution for each parameter after marginalizing over the two other. Figure 1(d) shows the most likely profile given the data and uncertainty. The best value for each parameter matches the specified values well, with most likely values of $Te_0 = 1350$ eV, $\alpha = 8$, and $\beta = 8$.

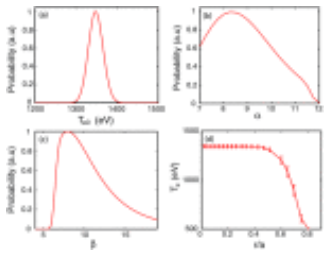


FIG. 1. Posterior probability distributions of Te_0 (a), α (b), and β (c) after marginalizing over the other two parameters. (d) The most likely profile after marginalizing over α and β . The error bars are the $1-\sigma$ uncertainty in the marginalized temperature.

While this work concentrates on axi-symmetric plasmas with no structure, MST has the capability to sustain various temperature structures, and future development aims to include such structure. Including structure, however, necessitates many more parameters making a grid search impractically time-consuming, so we aim to use Markov chain Monte-Carlo (MCMC) methods for that analysis.^{13,14} A MCMC analysis of the three parameter profile describe by Eq. (5) is implemented here so that it can be compared to the grid search. Slice sampling for the MCMC is chosen to take advantage of its ability to accurately estimate the whole distribution, even in the case of strong covariance or multimodal distributions,¹⁵ as the measurement uncertainty is derived from the full distribution. Some care has been spent varying the settings of the MCMC using the synthetic data to examine stability and accuracy.

Of particular importance for distribution stability is the width of the region around each parameter that the MCMC searches to choose the next value in the Markov chain. The widths for each parameter have been tuned such that a trace of all choices for a single parameter appears as close to random noise as possible. The number of samples kept in the chain was set such that the addition of five times more samples did not significantly change the distribution for any parameter. These criteria ensure stable and accurate distributions, as seen by the agreement between the grid search and the MCMC analysis, shown in Fig. 2.

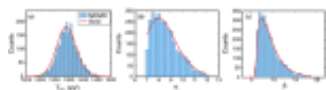


FIG. 2. Agreement between distributions for Te_0 (a), α (b), and β (c) after marginalizing over the other two parameters for the grid search (solid red curve) and the MCMC analysis (bars).

Also of importance are the choices for the prior probabilities. As noted, the MCMC analysis reproduces the probability distribution well, however, a different choice of prior, even one as simple as changing the range of a uniform prior, can give rise to a bias in the most likely value or different distribution widths. In this case, for example, a larger range in α leads to a wider distribution for α as well as β , thus affecting the estimated uncertainty for both those parameters.

Marginalized distributions using a grid search for Te measurements from a single time point of experimental data for which no temperature structures are expected (i.e., Eq. (5) is a good model) are shown in Figs. 3(a)–3(c), which contains likelihood functions for SXR (red, dashed) and TS (blue, dashed-dotted) along with the resulting posterior distributions (green, solid). Note the maximum in the posterior distribution occurs where the two likelihoods overlap. The most likely parameters are $Te_0 = 1425$ eV, $\alpha = 8$, and $\beta = 15$, and the most likely profile is shown in Fig. 3(d). This is the profile for Te that is the most consistent with both sets of data after marginalizing over α and β . For this shot, the SXR

system is clearly a weak constraint. This is because the temperature is largely constant over region where the majority of the SXR chords measure. Note that while in the core SXR and TS have uncertainties of about 100 eV and 150 eV, respectively, the integrated analysis value of T_e in the core has an uncertainty of about 30 eV. This dramatic increase in precision occurs because of the combination of data from both SXR and TS.

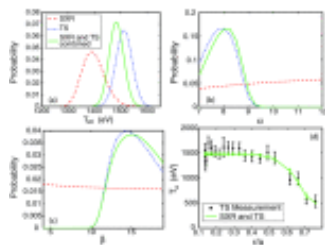


FIG. 3. Experimental results for the three parameters T_{e0} (a), α (b), and β (c) for a single shot. (a)–(c) The SXR likelihood is the red dashed line, the TS likelihood is the blue dashed-dotted line, and the integrated result is the solid green line. (d) The profile that is most consistent with both sets of data with the estimated 1- σ uncertainty (solid green line), compared to the measured TS data (the black stars). This profile has been marginalized over α and β .

A Bayesian probability theory based analysis of the double-foil SXR tomography temperature data has been implemented, and the integration of the SXR and TS diagnostics on MST has been demonstrated, yielding more precise measurements of electron temperature. The tomographic layout of the SXR system means that the TS and SXR system overlap poloidally, making the inclusion of structure a straightforward task, so we anticipate that this technique will be useful for analyzing temperature structures such as islands. We are also using this technique to explore the feasibility of measuring the effective ion charge in MST.

1. S. K. Rathgeber et al., *Plasma Phys. Control. Fusion* **52**, 095008 (2010).
<http://dx.doi.org/10.1088/0741-3335/52/9/095008>
2. B. Ph. van Milligen et al., *Rev. Sci. Instrum.* **82**, 073503 (2011).
<http://dx.doi.org/10.1063/1.3608551>
3. G. Verdoolaege, R. Fischer, and G. Van Oost, *IEEE Trans. Plasma Sci.* **38**, 3168 (2010).
<http://dx.doi.org/10.1109/TPS.2010.2071884>
4. D. Sivia, *Data Analysis: A Bayesian Tutorial*, 2nd ed. (Oxford University Press, New York, 2002).
5. M. B. McGarry, P. Franz, D. J. Den Hartog, and J. A. Goetz, *Rev. Sci. Instrum.* **81**, 10E516 (2010).
<http://dx.doi.org/10.1063/1.3481167>
6. M. B. McGarry, P. Franz, D. J. Den Hartog, J. A. Goetz, M. A. Thomas, M. Reyfman, and S. T. A.

- Kumar, *Rev. Sci. Instrum.* **83**, 10E129 (2012).<http://dx.doi.org/10.1063/1.4740274>
7. F. C. Jahoda, E. M. Little, W. E. Quinn, G. A. Sawyer, and T. F. Stratton, *Phys. Rev.* **119**, 843 (1960).<http://dx.doi.org/10.1103/PhysRev.119.843>
 8. T. P. Donaldson, *Plasma Phys.* **20**, 1279 (1978).<http://dx.doi.org/10.1088/0032-1028/20/12/005>
 9. J. Johnson, "Implementing Bayesian statistics and a full systematic uncertainty propagation with the soft X-ray tomography diagnostic on the Madison Symmetric Torus," Bachelor of Science thesis (University of Wisconsin-Madison, 2013).
 10. P. Franz, L. Marrelli, A. Murari, G. Spizzo, and P. Martin, *Nucl. Fusion* **41**, 695 (2001).
<http://dx.doi.org/10.1088/0029-5515/41/6/304>
 11. J. A. Reusch, M. T. Borchardt, D. J. Den Hartog, A. F. Falkowski, D. J. Holly, R. O'Connell, and H. D. Stephens, *Rev. Sci. Instrum.* **79**, 10E733 (2008).<http://dx.doi.org/10.1063/1.2956742>
 12. H. D. Stephens, D. J. Den Hartog, C. C. Hegna, and J. A. Reusch, *Phys. Plasmas* **17**, 056115 (2010).<http://dx.doi.org/10.1063/1.3388374>
 13. N. Metropolis, A. W. Rosenbluth, M. N. Rosenbluth, A. H. Teller, and E. Teller, *J. Chem. Phys.* **21**, 1087 (1953).<http://dx.doi.org/10.1063/1.1699114>
 14. W. K. Hastings, *Biometrika* **57**, 97 (1970).<http://dx.doi.org/10.1093/biomet/57.1.97>
 15. D. M. Higdon, *J. Am. Stat. Assoc.* **93**, 585 (1998).
<http://dx.doi.org/10.1080/01621459.1998.10473712>

© 2014 AIP Publishing LLC

Recently Viewed Content

Note: Effect of photodiode aluminum cathode frame on spectral sensitivity in the soft x-ray energy band